Microchimica Acta (2019) 186: 755
https://doi.org/10.1007/s00604-019-3940-5

ORIGINAL PAPER

Rapid colorimetric determination of dopamine based on the inhibition of the peroxidase mimicking activity of platinum loaded $CoSn(OH)_6$ nanocubes

Hao Liu[1] · Ya-Nan Ding[1] · Bing Bian[1,2] · Lei Li[3,4] · Ruomeng Li[1] · Xianxi Zhang[3,4] · Zhenxue Liu[1] · Xiao Zhang[2] · Gaochao Fan[2] · Qingyun Liu[1]

Received: 23 June 2019 / Accepted: 12 October 2019 / Published online: 9 November 2019

Abstract

Platinum nanoparticles were loaded on CoSn(OH)6 nanocubes via a co-precipitation method. The material (NCs) is shown to be a viable peroxidase mimic that catalyzes the oxidation of 3,3′,5,5′-tetramethylbenzidine (TMB) by hydrogen peroxide (H_2O_2) to generate oxidized TMB (oxTMB) with absorption at 652 nm. The formation of the blue color can be observed in <30 s. Thus, a visual and colorimetric assay was worked out for H_2O_2. It has a detection limit as low as 4.4 μM and works in the 5 to 200 μM concentration range. The method was also used to detect dopamine (DA) which is found to inhibit the enzyme mimicking activity of the NCs. Hence, less blue color is formed in its presence. The respective DA assay has a linear response in the 5.0 to 60 μM concentration range and a 0.76 μM detection limit.

Keywords Synergistic effect · Co-precipitation · Antioxidants · Inhibition · Catalytic mechanism · Serum

Introduction

Dopamine (DA) as a catecholamine neurotransmitter plays a crucial part in cardiovascular and renal systems of humans and mammals [1]. The abnormal levels of the DA may cause people to suffer from Parkinson disease and cardiovascular diseases [2, 3]. Thus, developing a method to detect DA is significance. As we know, the detection of DA is usually performed using electrochemical methods owing to the excellent electrochemical properties of DA [3]. However, the electrochemical detection of DA at the solid electrode is easy interfered by the co-existence of UA (uric acid) and ascorbic acid (AA). Because they also may be oxidized more or less at the same potential, and which would cause the overlapping voltammetric response [4, 5]. Besides the electrochemical method, the detection of DA is usually performed using high-resolution chromatography [6], fluorescent [7] and chemiluminescence [8] methods. Compared above these methods, colorimetry has been widely aroused attention because of its more cost effectiveness, convenience of visual observation and simplicity [9, 10]. However, DA detection remain has some restrictions, including the low selectivity and sensitivity, high detection limits and complex operating process. Thus, in order to solve these problems, establishing a sensitive and rapid DA detection platform is quite important for clinical diagnosis and physiology research.

Up to now, a variety of nanozymes [11, 12] have been widely reported. Among these nanozymes, Platinum nanoparticles (Pt NPs) and their hybrids have received extensive attention due to their effective catalytic activity [13, 14]. By

Electronic supplementary material The online version of this article (https://doi.org/10.1007/s00604-019-3940-5) contains supplementary material, which is available to authorized users.

✉ Qingyun Liu
qyliu@sdust.edu.cn

[1] College of Chemical and Environmental Engineering; State Key Laboratory of Mining Disaster Prevention and Control Co-founded by Shandong Province and the Ministry of Science and Technology, Shandong University of Science and Technology, Qingdao 266590, China

[2] College of Chemistry and Molecular Engineering, Qingdao University of Science & Technology, Qingdao 266042, China

[3] Shandong Provincial Key Laboratory/Collaborative Innovation Center of Chemical Energy Storage & Novel Cell Technology, Liaocheng University, Liaocheng 252059, China

[4] School of Chemistry and Chemical Engineering, Liaocheng University, Liaocheng 252059, China

calculating adsorption energies and activation energies, Li et.al found that Au, Ag and Pt catalyze H_2O_2 decomposition reaction rate followed the order Au (111) < Ag (111) < Pt (111) in equal acidic conditions [13]. In addition, compared with Rhodium and Iridium nanoparticles, platinum nanoparticles exhibit more advantages, such as available raw materials, more environmental friendliness, large surface and hypotoxicity, etc. Nevertheless, Pt NPs tend to aggregate in the solution, resulting in the reduction of the catalytic activity. Anchoring of metal particles on a special carrier is thought as an effective way to both prevent the aggregation and keep the catalytic activity of the metal NPs [14]. Thus, $CoSn(OH)_6$, as one of perovskite materials, is selected as a support to control Pt NPs without using capping agents due to its large specific surface areas, high catalytic activities and potential for high loading capacity [15, 16]. In addition, $CoSn(OH)_6$ provides more adsorption sites and active sites, benefiting the affinity between NCs and substrate as well as the catalytic activity of NCs.

Herein, we provided a two-step co-precipitation strategy to prepare NCs with the high peroxidase-like activity. The NCs can catalyze the oxidation of TMB to yield blue oxTMB by H_2O_2 in less than 30 s. Thus, a superior and high sensitivity colorimetric platform based on NCs was established and firstly used to detect H_2O_2. The catalytic mechanism is attributed to hydroxyl radical produced in the catalytic process, which verified by a fluorescence probe. In addition, the colorimetric method displays the superior sensitivity and selectivity for detection of DA.

Experimental section

Chemicals and materials

All reagents are of analytical grade. $Co(NO_3)_2$•$6H_2O$, sucrose, $NaBH_4$, terephthalic acid (TA), Trisodium citrate dihydrate and $SnCl_4$•$5H_2O$ were ordered from Guangcheng Reagent Co., Ltd. (Tianjin, China, http://sp2677674.zjbiz.net/). TMB•2HCl, K_2PtCl_4, D-Histidine, Dopamine, L-Arginine, D-serine, DL-Isoleucine, Uric acid, L-cysteine, Glutathione, Ascorbic acid and DL-Tryptophan were ordered from Sigma-Aldrich (St. Louis, MO, www.sigmaaldrich.com/). The human serum samples were gained from two healthy volunteers at the affiliated Hospital of Qingdao University (Qingdao, China, http://www.qduh.cn/), and informed consents were gained from two healthy volunteers. All assays were tested in accordance with the relevant institutional guidelines, and approved by the Ethics Committee of Qingdao University.

Characterization of $CoSn(OH)_6$ and Pt/$CoSn(OH)_6$ nanocubes (NCs)

$CoSn(OH)_6$ was synthesized via a modified precipitation strategy [16]. The details of the preparation of $CoSn(OH)_6$ and Pt/$CoSn(OH)_6$ NCs are shown in the Supporting Information (SI). $CoSn(OH)_6$ and Pt/$CoSn(OH)_6$ NCs were characterized by X-ray diffraction (XRD) pattern (Japan, https://www.rigaku.com/en), transmission electron microscopy (TEM, JEOL, Japan https://www.jeol.co.jp/), bright field scanning transmission electron microscopy (BF-STEM), high angle annular dark field scanning transition electron microscopy (HAADF-STEM), EDS mapping (JEOL, Japan, https://www.jeol.co.jp/), X-ray photoelectron spectra (XPS) (USA, https://www.thermofisher.com), and inductively coupled plasma atomic emission spectroscopy (ICP-AES, USA, https://www.perkinelmer.com.cn). The fluorescence spectra and UV-visible absorbance of reaction system were tested by Hitachi F-4600 FLSPECTROPHOTOMET spectrophotometer (Tokyo, Japan, http://www.hitachi.com/) and UV-1810 PC spectrophotometer (Beijing General Analysis Instrument Co., Ltd. http://www.pgeneral.com), respectively. The specific details are present in the Supporting Information.

Peroxidase-like activity of NCs

The peroxidase mimetic activity of the NCs was tested by selecting TMB as a chromogenic substrate in the presence of H_2O_2 to generate oxidized TMB (oxTMB) with absorption at 652 nm [17–19]. The measurement procedure was described as follows: 200 μL 0.06 mg·mL^{-1} NCs, 1400 μL of acetate buffer (pH = 4.0), 200 μL of 1 mM TMB and 200 μL of 0.25 M H_2O_2 were added into each well, and the system absorbance was monitored by a UV-1810 PC spectrophotometer at 652 nm after reacting for 3 min. The effects of different reaction conditions such as pH (2.0~9.0) and temperature (20~70 °C) on the peroxidase mimetic activity of NCs were verified by the same procedures mentioned above. Furthermore, the peroxidase mimetic of the different Pt/$CoSn(OH)_6$ systems was also tested under the same assay conditions. Steady-state kinetic assay detail of NCs is shown in the Supporting Information (SI).

H_2O_2 assay

The colorimetric detection of H_2O_2 was performed by adding 200 μL 0.06 mg·mL^{-1} Pt/$CoSn(OH)_6$ and 200 μL of 1 mM TMB to 1400 μL of acetate buffer (pH = 4.0). After adding different concentrations H_2O_2 solution (5–1000 μM) to the above mixture for 3 min, the absorbance was recorded at 652 nm by UV-1810 PC spectrophotometer. The limit of detection (LOD) was calculated by formula LOD = 3 s/k, where s, k are the relative standard deviation of eight parallel controlled measurements and the slope of the linear calibration plots, respectively.

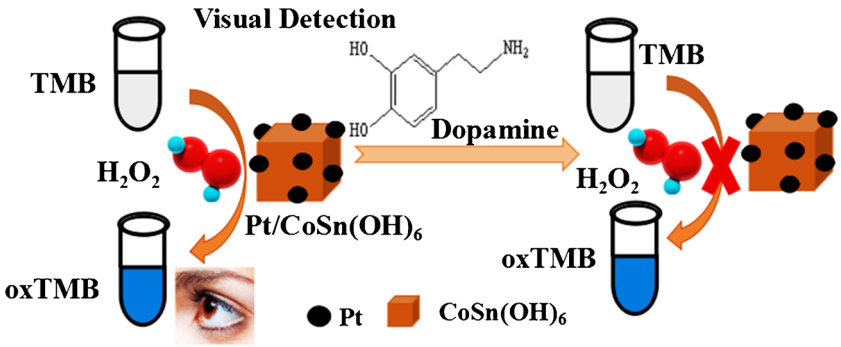

Scheme 1 The schematic diagram of detection of H_2O_2 and dopamine based on the inhibition of the peroxidase-like activity of $Pt/CoSn(OH)_6$

Dopamine assay

The dopamine detection system was performed by adding 200 μL 0.06 mg·mL^{-1} $Pt/CoSn(OH)_6$, 200 μL of 1 mM TMB and 200 μL different concentrations DA solution (0–100 μM) to 1200 μL of acetate buffer (pH = 4.0). After adding 200 μL H_2O_2 (0.25 M) to the above mixture for 3 min, the absorbance was recorded at 652 nm by UV-1810 PC spectrophotometer. The selectivity assays for DA detection was carried out by adding 200 μL 0.06 mg·mL^{-1} $Pt/CoSn(OH)_6$, 200 μL of 1 mM TMB and 200 μL different interferences such as 200 μM D-Histidine, Sucrose, L-Arginine, D-serine, DL-Isoleucine and DL-Tryptophan as well as 20 μM Uric acid, L-cysteine, Glutathione and Ascorbic acid in lieu of 20 μM DA to 1200 μL of acetate buffer (pH = 4.0). After adding 200 μL H_2O_2 (0.25 M) to the above mixture for 3 min, the absorbance was recorded at 652 nm by UV-1810 PC spectrophotometer.

Results and discussion

Choice of materials

$CoSn(OH)_6$, as a well-defined three dimensional (3D) perovskite-type material, has excellent electromagnetic properties, large specific surface areas, high catalytic activities and potential for high loading capacity. Thus, large specific surface areas of $Pt/CoSn(OH)_6$ NCs not only can provide abundant loading sites with Pt NPs to prevent the aggregation of Pt

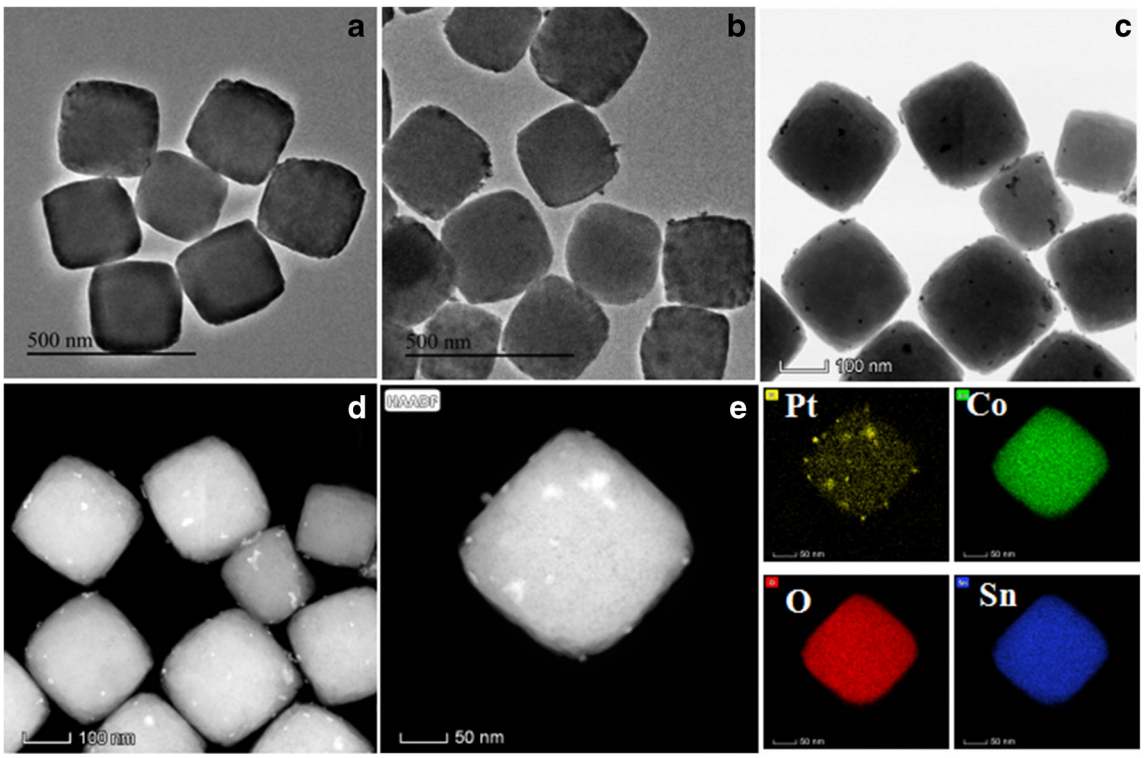

Fig. 1 The TEM images of $CoSn(OH)_6$ and $Pt/CoSn(OH)_6$ (**a**–**b**), BF-STEM and HAADF-STEM image of $Pt/CoSn(OH)_6$ (**c**–**d**), EDX-HAADF-Mapping images of Pt, Cu, O and Sn elements (**e**)

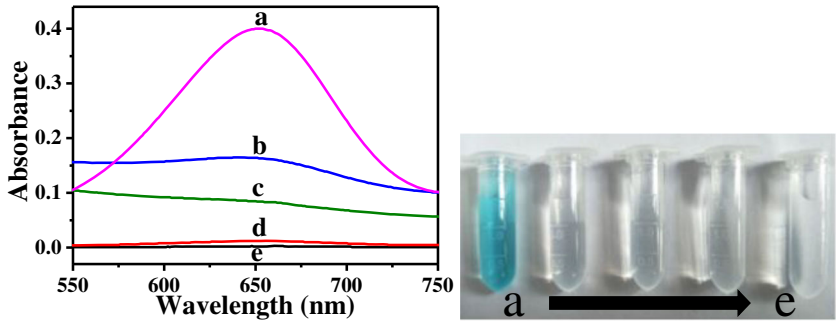

Fig. 2 UV-vis spectra of TMB (200 μL, 1 mM) and with and without H_2O_2 (200 μL, 0.25 M) with different catalysts (200 μL 0.06 mg·mL^{-1} NCs or 200 μL 0.06 mg·mL^{-1} $CoSn(OH)_6$ NCs): (a-e) H_2O_2 + TMB + Pt/$CoSn(OH)_6$, H_2O_2 + TMB + $CoSn(OH)_6$, Pt/$CoSn(OH)_6$ + TMB, H_2O_2 + TMB, alone TMB, and the corresponding photos of color changes (3 min, a-e)

NPs, but also NCs can provide more adsorption sites and active sites, benefiting to decompose absorbed H_2O_2 into •OH. Highly dispersed Pt NPs loaded on $CoSn(OH)_6$ means that more catalytic sites of Pt NPs are exposed to enhance the catalytic activity of Pt NPs. Excellent semiconductor performance of $CoSn(OH)_6$ also accelerates electron transfer between OH• radicals and TMB to accelerate reaction rates. Even if a large amount of enzyme-mimicking nanomaterials were reported with great catalytic activity [20]. To further illuminate the catalytic mechanism of enzyme-mimicking nanomaterials and improve selectivity and convenience for detection DA and H_2O_2, developing a novel mimetic enzyme with excellent catalytic activity is of great significance. Thus, the colormetric platform based on the peroxidase-like activity of NCs has been designed to detect DA and H_2O_2, and the schematic diagram of DA and H_2O_2 detection is shown in Scheme 1.

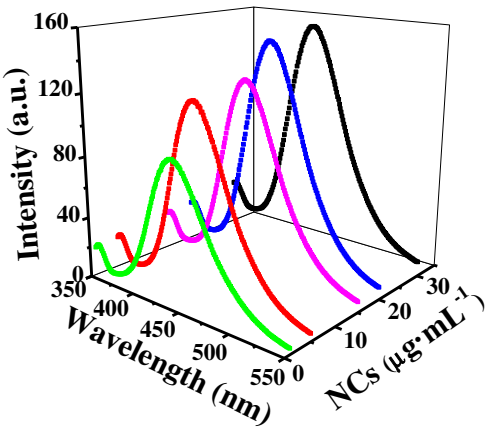

Fig. 3 The Fluorescence spectra of reaction system due to decomposition of H_2O_2 by Pt/$CoSn(OH)_6$ catalyzing with different concentration: 1, 5, 15, 20 and 30 μg·mL^{-1}, respectively. The reaction system including of 200 μL different concentrations NCs (1, 5, 15, 20 and 30 μg·mL^{-1}), H_2O_2 (200 μL, 0.25 M), TA (200 μL, 5 mM) and 1400 μL of acetate buffer (pH = 4.0) was incubated at 45 °C for 20 min

Characterization of materials

The crystalline structures of samples tested by XRD are shown in Fig. S1. The all diffraction are attributed to $CoSn(OH)_6$ (JCPDS card No. 13–0356), corresponding to (111), (200), (220), (310), (311), (222), (400), (420), (422), (511), (440), (442) and (620) planes, respectively. However, the diffraction peak of Pt (JCPDS card No. 04–0802) is not found, due to the low loading content or the high dispersion of Pt in $CoSn(OH)_6$. The Pt content is determined to be 0.05 wt.% by ICP, listed in Table S1. Notably, the crystalline form of $CoSn(OH)_6$ is not changed and no other diffraction peaks generate after loading Pt.

Figure 1a, b show the TEM images of $CoSn(OH)_6$ and Pt/$CoSn(OH)_6$ NCs, respectively. Compared with that of $CoSn(OH)_6$, highly dispersed Pt NPs can be imaged by BF-STEM and HAADF-STEM (Fig. 1c, d). As can be seen from Fig. 1e, the Sn, Co and O elements exist homogenously in NCs. In contrast, the distribution of Pt NPs is discrete, indicating a hierarchical heterostructure with good dispersion on the surface of $CoSn(OH)_6$ nanocubes.

All the surface elements chemical states of NCs are verified by XPS analysis, shown in Fig. S2a. The Pt 4f signal spectrum consists of dual doublets by deconvoluting the spectra (Fig. S2b). The peaks of metallic Pt can be seen at 70.7 and 73.9 eV. The two main peaks of Co 2p XPS survey spectrum at 780.6 and 796.5 eV are corresponding to Co $2p_{3/2}$ and Co $2p_{1/2}$ (Fig. 2c), which are typical XPS diffraction peak of Co^{2+}, accompanied by satellite peaks [21]. The intensity of the satellite peaks for two samples is very strong, indicating that the Co element exists in the NCs with the oxidation state of +2 [22]. The two strong XPS peaks of Sn 3d at 486.1 and 494.3 eV (Sn $3d_{3/2}$ and Sn $3d_{5/2}$) are attributed to the electronic state of Sn^{4+} (Fig. S2d). The XPS peak of O1s is located at ~530.7 eV, assigned to the hydroxyl groups with metal ion of $CoSn(OH)_6$ [23] (Fig. S2e). The C1s XPS signal is used to calibrate binding energies, shown in Fig. S2f. The above XRD, TEM, STEM and XPS results verify the successful preparation of NCs.

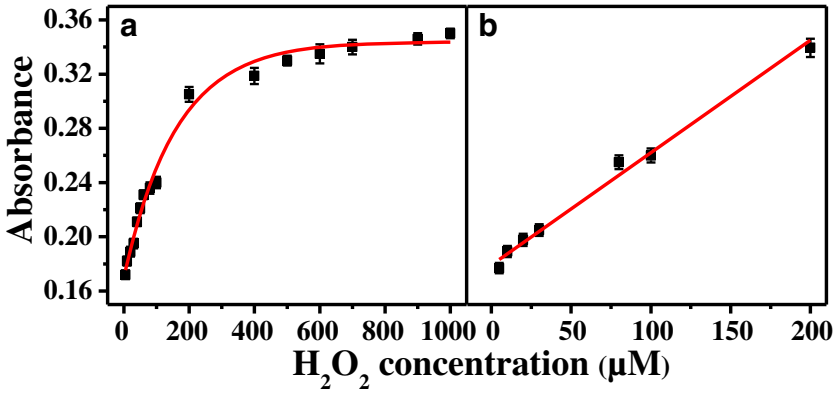

Fig. 4 **a** The response curve of variable concentration of H_2O_2 (5–1000 μM) towards the peroxidase-like activity of Pt/$CoSn(OH)_6$ (0.06 mg·mL^{-1}) in presence of TMB (1 mM) and **b** the linear calibration plot for H_2O_2 detection, respectively

Peroxidase-like activity assays results of NCs

The peroxide mimetic enzyme activity of NCs was characterized by selecting TMB as a colorimetric substrate with or without H_2O_2. As can be seen from Fig. 2, the TMB exhibits negligible absorbance and no color change without or only with H_2O_2 (curve d and e). The color of TMB (curve c) is not changed without H_2O_2, even if NCs are added. After adding pure $CoSn(OH)_6$ NCs into the solution of TMB and H_2O_2, a negligible absorption (curve b) with a weak color change can be found. Nevertheless, the NCs display a stronger absorption at 652 nm with an obvious color change (curve a), revealing the superior peroxidase-like activity. Compared the response time with other nanoenzymes, it is clearly seen that NCs demonstrate the high catalytic efficiency under the lower concentration of TMB (1 mM), listed in Table S2. In other words, all the results described above indicate that NCs can efficiently catalyze the oxidation of TMB to produce charge-transfer complex (oxTMB) with H_2O_2 [18, 19].

To investigate how pH and temperature affect the catalytic activity of NCs, the optimal experiments were conducted in different pH (2–9) and temperature (20–70 oC), respectively. From Fig. S3a, we can clearly observe that NCs exhibit the maximum activity at pH = 4.0. Whether the value of pH is lower or higher than 4, the catalytic activity is reduced. The oxidation of TMB can be suppressed at pH < 3, because H_2O_2 may be divided into H_2O and O_2 rather than reactive oxygen species (ROS) in high pH [24]. The influence of experimental temperature was also studied. The optimal temperature of the catalytic system is 45 °C (Fig. S3b). Importantly, the peroxide-like activity of NCs is always >70% in the temperature range of 20–70 °C, revealing the superior stability of the NCs, compared with that of reported artificial nanozymes and natural enzymes.

Catalytic mechanism of nanocubes (NCs)

Previous reports indicate that the catalytic mechanism of peroxide mimics is mainly classified into two types: OH• radicals [25] and electron transfer [26]. To verify the catalytic mechanism of NCs, we chose TA as a fluorescent probe to catch the produced hydroxyl radicals during the catalytic reaction. Terephthalic acid can react with hydroxyl radicals to form fluorescent 2-hydroxyterephthalic acid with the fluorescence emission wavelength at 435 nm [12, 25]. The fluorescence intensity increased continuously with increasing of added NCs from 1 to 30 μg mL^{-1}, indicating that the production of OH• (Fig. 3). As a result, NCs catalyze the degradation of H_2O_2 to yield OH•, which can rapidly oxidize TMB into a blue oxTMB.

Table 1 Comparison of detection limit of H_2O_2 based on different nanoenzymes with different detection method

Nanomaterials	Method	LOD	Ref.
Prussian-blue/graphite-composite	Batch injection	10 μM	[28]
Pt nanoparticles/carbon nanotubes	Flow injection	20 μM	[29]
PtCu NWs	Colorimetry	0.06 μM	[30]
C-dot/V_2O_5	Colorimetry	0.5 μM	[31]
PDI-CeO_2 NC	Colorimetry	2.59 μM	[32]
Fe/$CuSn(OH)_6$ microspheres	Colorimetry	9.49 μM	[25]
Pt/$CoSn(OH)_6$	Colorimetry	4.42 μM	This work

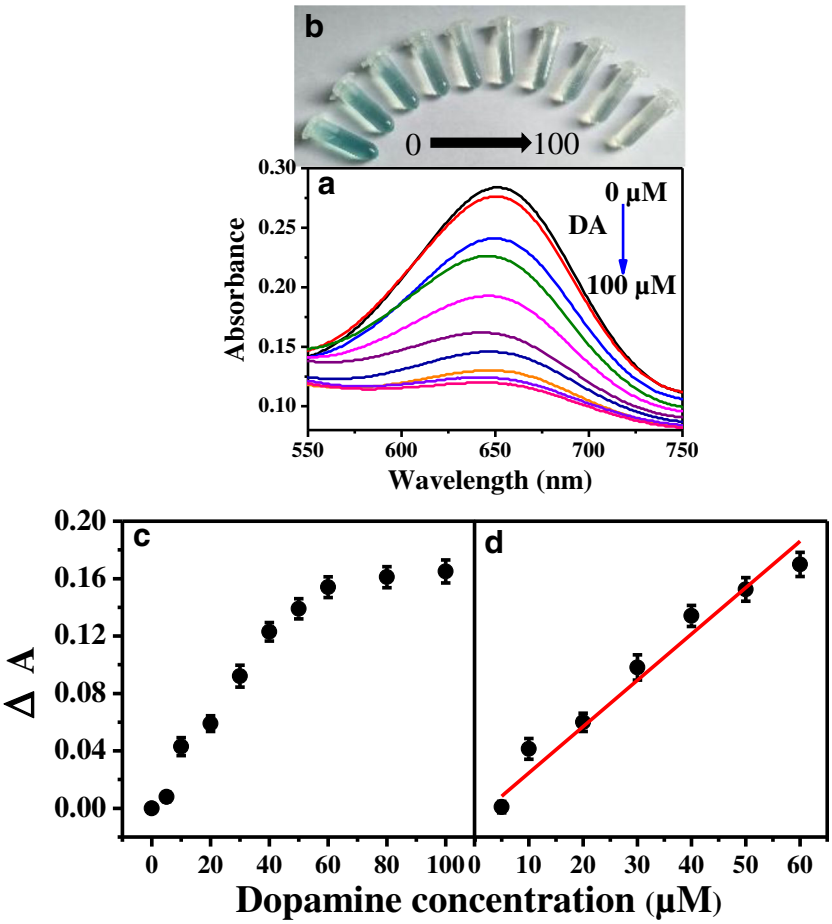

Fig. 5 **a** UV-vis absorption spectra of TMB-H_2O_2-Pt/$CoSn(OH)_6$ colorimetric system composing of 200 μL of 0.06 mg·mL^{-1} NCs, 1 mM TMB, 0.25 M H_2O_2, different concentrations of dopamine (200 μL of 0, 5, 10, 20, 30, 40, 50, 60, 80, 100 μM) and 1200 μL of acetate buffer (pH = 4.0); **b** the corresponding photographs of above reaction; **c** The changes of reaction system's absorbance with addition of dopamine, and **d** the corresponding calibration plot for dopamine

Steady-state kinetic assay

To further investigate the peroxidase-like activity of NCs, steady-state kinetics are studied by selecting either TMB or H_2O_2 as a substrate. A series of experiment data and Michaelis-Menten curves were obtained by keeping the concentration of one substrate unchanged while varying the other. The results are corresponded to the Michaelis-Menten model of enzyme kinetics (Fig. S4). The values of Michaelis-Menten constant (K_m) and the maximum initial velocity (V_{max}) are evaluated by double-reciprocal Line weaver-Burk plots. The affinity between an enzyme and substrates is evaluated by K_m value. A smaller K_m value means a better affinity between nanoenzyme and substrates, and vice versa [17, 27]. From the data listed in Table S3, it can be observed that the K_m value of NCs and other nanomaterials-based enzyme mimics with H_2O_2 and TMB are smaller than that of HRP. It is suggested that NCs and other nanoenzyme mimics have a much stronger affinity to H_2O_2 and TMB than that of HRP.

Colorimetric determination of H_2O_2

Based on the peroxidase activity of NCs, an excellent colorimetric assay is constructed and used to detect H_2O_2. The experimental data are performed by an UV-vis spectrometer at 652 nm. A wider linear response range for H_2O_2 detection is from 5 to 200 μM with a detection limit of 4.42 μM (S/*N* = 3, Fig. 4). Table 1 lists the detection limit of H_2O_2 based on the NCs and different nanoenzymes by different methods. From the data, a smaller limit detection of H_2O_2 was found using

Table 2 Results of H_2O_2 detection in Lens care solution samples

Lens care solution samples	Detected (M)	Add (10^{-6} M)	Found (10^{-6} M)	Recovery (%)	RSD % (*n* = 3)
1	ND	20	20.16	100.78	1.13
2	ND	40	38.21	95.52	1.23
3	ND	60	58.22	97.01	1.17

ND No detection

Table 3 Results of DA detection in human serum samples

Samples[a]		Detected (M)	Add (10^{-6} M)	Found (10^{-6} M)	Recovery (%)	RSD % ($n = 3$)
Human serum 1	1	ND	15	14.77	98.49	1.72
	2	ND	20	20.51	102.54	1.24
	3	ND	30	30.19	100.62	0.84
Human serum 2	1	ND	20	20.12	100.60	1.78
	2	ND	30	28.90	96.34	1.24
	3	ND	40	36.91	92.27	1.11

[a] Human serum samples were provided by the affiliated Hospital of Qingdao University (Qingdao, China)

NCs than that using other nanoenzymes (such as Prussian-blue/graphite-composite [28], Pt nanoparticles/carbon nanotubes [29] and Fe/$CuSn(OH)_6$ microspheres [25]), and the detection limit of H_2O_2 using NCs together with another nanoenzymes in previous publications [30–32] are relatively low, indicating a good sensitivity of our colorimetric assay.

Determination of dopamine

According the previous studies [33], Dopamine can inhibit the peroxidase-like activity and result in fluorescence quenching. Because dopamine inhibits the catalytic oxidation of TMB, the colorimetric method was performed to detect dopamine. It can be clearly observed that the absorbance of the system reduces gradually with the increase of DA. The color of the system varies gradually from blue color to colorless, shown in Fig. 5a, b. The results indicate that DA can restrain the catalytic oxidation of TMB. The activity of OH• radicals is quenched by the DA, accordingly curbing the oxidation of TMB [34]. The response curve between DA concentration and absorbance is shown in Fig. 5c, d. The value of ΔA is calculated by the following formula: $\Delta A = A_{Blank} - A$ (A and A_{Blank} represent the absorbance values of the reaction system at 652 nm with and without DA, respectively). The linear range is from 5 to 60 μM and detection limit of DA is calculated to be 0.76 μM ($S/N = 3$, LOD = 3 s/k, where s, k are the relative standard deviation of eight parallel controlled measurements and the slope of the linear calibration plots, respectively.), which is superior to previous reports listed in Table S4, indicating the excellent sensitivity of our assay for detection of DA.

Selectivity test result of dopamine detection

It is pointed out that colorimetric method for detecting DA should be considered for the interference of other antioxidants such as L-cysteine, Glutathione and Ascorbic acid when analyzing real samples coexist in complex systems. Thus, the selectivity was performed with DA (20 μM) and other interfering substances (200 μM D-Histidine, Sucrose, L-Arginine, D-serine, DL-Isoleucine and DL-Tryptophan, 20 μM Uric acid, L-cysteine, Glutathione and Ascorbic acid). The experimental results are displayed in Fig. S5. Compared with that of other interfering substances together with antioxidants (L-cysteine, Glutathione and Ascorbic acid), our colorimetric platform has the highest relative ΔA absorbance $\left(\text{Relative } \Delta A \text{ absorbance} = \frac{\Delta A(\text{Interfering substance})}{\Delta A(\text{dopamine})} \times 100\%\right)$ at 652 nm, indicating the excellent selectivity of the colorimetric method for DA.

Determinations of H_2O_2 and dopamine in real samples

To explore the potentiality of practical application, the established colorimetric platform was used to determinate H_2O_2 in lens care solution and DA in human serum samples by the standard addition method, respectively. The detection results are listed in Tables 2 and 3. The recoveries for H_2O_2 are ranged between 95.52–100.78% with relative standard deviation (RSD) of 1.15–2.29%. No H_2O_2 was detected in lens care solution samples.

In addition, the recoveries of DA detection in Human serum 1 and 2 are 98.5–102.5% with the RSDs of 0.8–1.7% as well as 92.3–100.6% with the RSDs of 1.1–1.8%, respectively. Similarly, no dopamine was detected in two serum samples. The above results indicate that our method exhibit credibility and repeatability for detection of H_2O_2 and DA in real samples (Tables 2 and 3).

Conclusions

The highly dispersed Pt-loaded $CoSn(OH)_6$ NCs were successfully synthesized. The NCs exhibit the superior mimic peroxidase performance, ascribed to production of •OH under the synergetic effect between Pt and $CoSn(OH)_6$. The catalytic activity of the NCs is higher even at higher temperature. Base on the peroxidase-like activity of NCs, a colorimetric detection platform was successfully established and used to detect H_2O_2 and DA, respectively. The colorimetric platform exhibited favorable selectivity toward DA and successfully used in the detection of H_2O_2 and DA in real samples. The novel, visual, rapid, high stability and sensitive nanoprobe has a

potential application in nanotechnology, medical analysis and biosensors.

Acknowledgments This work was supported by the National Natural Science Foundation of China (Grant No. 21971152), Scientific Research Foundation of Shandong University of Science and Technology for Recruited Talents (Grant No. 2015RCJJ018, 2017RCJJ040 and 2017RCJJ041), Natural Science Foundation of Shandong Province (Grant No. ZR2018MB002, ZR2018MEE003, ZR2018PEE006 and ZR2017BB008), the Science and Technology Projects for Colleges and Universities in Shandong Province (No. J17KA097) and Innovation Fund of Science & Technology of Graduate Students (SDKDYC180239).

Compliance with ethical standards

Conflict of interest The author(s) declare that they have no competing interests.

References

1. Zhang A, Neumeyer JL, Baldessarini RJ (2007) Recent Progress in development of dopamine receptor subtype-selective agents: potential therapeutics for neurological and psychiatric disorders. Chem Rev 107:274–302. https://doi.org/10.1021/cr050263h
2. Dawson TM, Dawson VL (2003) Molecular pathways of Neurodegeneration in Parkinson's disease. Science 302:819–822. https://doi.org/10.1126/science.1087753
3. Song H, Zhao H, Zhang X, Xu Y, Cheng X, Gao S, Huo L (2019) A hollow urchin-like α-MnO_2 as an electrochemical sensor for hydrogen peroxide and dopamine with high selectivity and sensitivity. Microchim Acta 186(4):210. https://doi.org/10.1007/s00604-019-3316-x2
4. Sumathi C, Raju CV, Muthukumaran P, Wilson J, Ravi G (2016) Au-Pd bimetallic nanoparticles anchored on α-Fe_2O_3 nonenzymatic hybrid nanoelectrocatalyst for simultaneous electrochemical detection of dopamine and uric acid in the presence of ascorbic acid. J Mater Chem B 4:2561–2569. https://doi.org/10.1039/C6TB00501B
5. Kumar SS, Mathiyarasu J, Phani KL (2005) Exploration of synergism between a polymer matrix and gold nanoparticles for selective determination of dopamine. J Electroanal Chem 578:95–103. https://doi.org/10.1016/j.jelechem.2004.12.023
6. Li N, Guo J, Liu B, Yu Y, Cui H, Mao L, Lin Y (2009) Determination of monoamine neurotransmitters and their metabolites in a mouse brain microdialysate by coupling high-performance liquid chromatography with gold nanoparticle-initiated chemiluminescence. Anal Chim Acta 645:48–55. https://doi.org/10.1016/j.aca.2009.04.050
7. Liu BW, Sun ZY, Huang PJ, Liu JW (2015) Hydrogen peroxide displacing DNA from nanoceria: mechanism and detection of glucose in serum. J Am Chem Soc 137:1290–1295. https://doi.org/10.1021/ja511444e
8. Zhao S, Huang Y, Shi M, Liu R, Liu YM (2012) Chemiluminescence resonance energy transfer-based detection for microchip electrophoresis. Anal Chem 82:2036–2041. https://doi.org/10.1021/ac9027643
9. Wu T, Hou W, Ma Z, Liu M, Liu X, Zhang Y, Yao S (2019) Colorimetric determination of ascorbic acid and the activity of alkaline phosphatase based on the inhibition of the peroxidase-like activity of citric acid-capped Prussian blue nanocubes. Microchim Acta 186:123. https://doi.org/10.1007/s00604-018-3224-5
10. Li ZM, Zhang X, Pi T, Bu J, Deng RH, Chi BZ, Zheng XJ (2019) Colorimetric determination of the activity of methyltransferase based on nicking enzyme amplification and the use of gold nanoparticles conjugated to graphene oxide. Microchim Acta 186:8. https://doi.org/10.1007/s00604-019-3690-4
11. Ding C, Yan Y, Xiang D, Zhang CL, Xian YZ (2016) Magnetic Fe_3S_4 nanoparticles with peroxidase-like activity, and their use in a photometric enzymatic glucose assay. Microchim Acta 183:625–631. https://doi.org/10.1007/s00604-015-1690-6
12. Dehghani Z, Hosseini M, Mohammadnejad J, Bakhshi B, Rezayan AH (2018) Colorimetric aptasensor for campylobacter jejuni cells by exploiting the peroxidase like activity of Au@Pd nanoparticles. Microchim Acta 185:448. https://doi.org/10.1007/s00604-018-2976-2
13. Li W, Bin C, Zhang HX, Sun YH, Wang J, Zhang JL, Fu Y (2015) BSA-stabilized Pt nanozyme for peroxidase mimetics and its application on colorimetric detection of mercury(II) ions. Biosens Bioelectron 66:251–258. https://doi.org/10.1016/j.bios.2014.11.032
14. Zhang LN, Deng HH, Lin FL, Xu XW, Weng SH, Liu AL, Lin XH, Xia XH, Chen W (2014) In situ growth of porous platinum nanoparticles on graphene oxide for colorimetric detection of cancer cells. Anal Chem 86:2711–2718. https://doi.org/10.1021/ac404104j
15. Takata T, Furumi Y, Shinohara K, Tanaka A, Hara M, Kondo JN, Domen K (1997) Photocatalytic decomposition of water on spontaneously hydrated layered perovskites. Chem Mater 9:1063–1064. https://doi.org/10.1021/cm960612b
16. Wang Z, Liu W, Xiao WX, Lou WD (2013) Amorphous $CoSnO_3$@C nanoboxes with superior lithium storage capability. Energy Environ Sci 6:87–91. https://doi.org/10.1039/C2EE23330D
17. Chen J, Chen Q, Chen J, Qiu H (2016) Magnetic carbon nitride nanocomposites as enhanced peroxidase mimetics for use in colorimetric bioassays, and their application to the determination of H_2O_2 and glucose. Microchim Acta 183(12):3191–3199. https://doi.org/10.1007/s00604-016-1972-7
18. Liu H, Ding Y, Yang B, Liu Z, Liu Q, Zhang X (2018) Colorimetric and ultrasensitive detection of H_2O_2 based on au/Co_3O_4-CeO_x nanocomposites with enhanced peroxidase-like performance. Sensors Actuators B-Chem 271:336–345. https://doi.org/10.1016/j.snb.2018.05.108
19. Liu QY, Yang YT, Li H, Zhu RR, Shao Q, Yang SG, Xu JJ (2015) NiO nanoparticles modified with 5, 10, 15, 20- tetrakis(4-carboxyl pheyl)-porphyrin: promising peroxidase mimetics for H_2O_2 and glucose detection. Biosens Bioelectron 64:147–153. https://doi.org/10.1016/j.bios.2014.08.062
20. Nasir M, Nawaz MH, Yaqub M, Hayat A, Rahim A (2017) An overview on enzyme-mimicking nanomaterials for use in electrochemical and optical assays. Microchim Acta 184:323–342. https://doi.org/10.1007/s00604-016-2036-8
21. Yang J, Liu H, Martens WN, Frost RL (2010) Synthesis and characterization of cobalt hydroxide, cobalt oxyhydroxide, and cobalt oxide nanodiscs. J Phys Chem C 114:111–119. https://doi.org/10.1021/jp908548f
22. Sahoo R, Sasmal AK, Ray C, Dutta S, Pal A, Pal T (2016) Suitable morphology makes $CoSn(OH)_6$ nanostructure a superior electrochemical pseudocapacitor. ACS Appl Mater Interfaces 8:17987–17998. https://doi.org/10.1021/acsami.6b02568
23. Volgmann K, Voigts F, Maus-Friedrichs W (2010) The interaction of oxygen molecules with iron films studied with MIES, UPS and XPS. Surf Sci 604:906–913. https://doi.org/10.1016/j.susc.2010.02.018
24. Nirala NR, Prakash R (2018) Quick colorimetric determination of choline in milk and serum based on the use of MoS_2 nanosheets as a

highly active enzyme mimetic. Microchim Acta 185(4):224. https://doi.org/10.1007/s00604-018-2753-2

25. Liu H, Ding YN, Yang B, Liu Z, Zhang X, Liu Q (2018) Iron doped $CuSn(OH)_6$ microspheres as a peroxidase-mimicking artificial enzyme for H_2O_2 colorimetric detection. ACS Sustain Chem Eng 6: 14383–14393. https://doi.org/10.1021/acssuschemeng.8b03082
26. Mu J, Wang Y, Zhao M, Zhang L (2012) Intrinsic peroxidase-like activity and catalase-like activity of Co_3O_4 nanoparticles. Chem Commun 48:2540–2542. https://doi.org/10.1039/c2cc17013b
27. Yang H, Yang R, Zhang P, Qin YM, Chen T, Ye FG (2017) A bimetallic (Co/2Fe) metal-organic framework with oxidase and peroxidase mimicking activity for colorimetric detection of hydrogen peroxide. Microchim Acta 184:4629–4635. https://doi.org/10.1007/s00604-017-2509-4
28. Silva RAB, Montes RHO, Richter EM, Munoz RAA (2012) Rapid and selective determination of hydrogen peroxide residues in milk by batch injection analysis with amperometric detection. Food Chem 133:200–204. https://doi.org/10.1016/j.foodchem.2012.01.003
29. Reanpang P, Themsirimongkon S, Saipanya S, Chailapakul O, Jakmunee J (2015) Cost-effective flow injection amperometric system with metal nanoparticle loaded carbon nanotube modified screen printed carbon electrode for sensitive determination of hydrogen peroxide. Talanta. 144:868–874. https://doi.org/10.1016/j.talanta.2015.07.041
30. Sui N, Li S, Wang Y, Zhang Q, Liu S, Bai Q, William WY (2019) Etched PtCu nanowires as a peroxidase mimic for colorimetric determination of hydrogen peroxide. Microchim Acta 186:186. https://doi.org/10.1007/s00604-019-3293-0
31. Honarasa F, Kamshoori FH, Fathi S, Motamedifar Z (2019) Carbon dots on V_2O_5 nanowires are a viable peroxidase mimic for colorimetric determination of hydrogen peroxide and glucose. Microchim Acta 186(4):234. https://doi.org/10.1007/s00604-019-3344-6
32. Lian J, Liu P, Jin C, Shi Z, Luo X, Liu Q (2019) Perylene diimide-functionalized CeO_2 nanocomposite as a peroxidase mimic for colorimetric determination of hydrogen peroxide and glutathione. Microchim Acta 186(6):332. https://doi.org/10.1007/s00604-019-3439-0
33. Chen JL, Yan XP, Meng K, Wang SF (2011) Graphene oxide based photoinduced charge transfer label-free near-infrared fluorescent biosensor for dopamine. Anal Chem 83:8787–8793. https://doi.org/10.1021/ac2023537
34. Nagvenkar AP, Gedanken A (2016) $Cu_{0.89}Zn_{0.11}O$, a new peroxidase-mimicking nanozyme with high sensitivity for glucose and antioxidant detection. ACS Appl Mater Interfaces 8:22301–22308. https://doi.org/10.1021/acsami.6b05354